12
Research paper I Оригинални научни рад
DOI 10.7251/STP2215112B
ISSN 2566-4484

Aleksandar Borković, University of Banja Luka, Graz University of Technology, aleksandar.borkovic@aggf.unibl.org
Dijana Majstorović, University of Banja Luka, dijana.majstorovic@aggf.unibl.org
Snježana Milovanović, University of Banja Luka, snjezana.milovanovic@aggf.unibl.org
Duy Vo, Thammasat University and Department of Civil and Environmental Engineering, Tokyo Institute of Technology, duyvo.ce@gmail.com

FREE VIBRATION ANALYSIS OF SINGLY CURVED CLAMPED SHELLS USING THE ISOGEOMETRIC FINITE STRIP METHOD

Abstract

A hybrid method for the spatial discretization of two-dimensional domains is recently derived and applied to the problem of free vibrations of simply-supported singly curved shells. This new method follows from a tensor product of NURBS functions and a carefully selected series that satisfies boundary conditions a priori. The formulation unifies spatial discretization schemes of the semi-analytical Finite strip method and the Isogeometric analysis. In this paper, the method is improved by implementing the capability to deal with clamped-clamped boundary conditions. The numerical analysis shows that the method has favorable accuracy per DOF, in comparison with the standard finite elements.

Keywords: Isogeometric analysis, finite strips, singly curved clamped shells, free vibrations

АНАЛИЗА СЛОБОДНИХ ВИБРАЦИЈА ЈЕДНОСТРУКО ЗАКРИВЉЕНИХ УКЉЕШТЕНИХ ЉУСКИ ПРИМЈЕНОМ ИЗОГЕОМЕТРИЈСКОГ МЕТОДА КОНАЧНИХ ТРАКА

Сажетак

Хибридни метод за просторну дискретизацију дводимензионалних домена је недавно изведен и примијењен на проблем слободних вибрација једноструко закривљених слободно ослоњених љуски. Поступак је заснован на тензорском производу НУРБС функција и пажљиво одабраних редова који а приори задовољавају граничне услове. Формулација обједињује два приступа просторне дискретизације домена: полуаналитички метод коначних трака и изогеометријску анализу. Кроз овај рад, метод је унапређен увођењем граничних услова укљештења. Нумеричка анализа показује да метод пружа одличан однос тачности рјешења и броја степени слободе, у поређењу са стандардним коначним елементима.

Кључне ријечи: изогеометријска анализа, коначне траке, једноструко закривљене укљештене љуске, слободне вибрације

1. INTRODUCTION

Singly curved shells are readily found in engineering structures in the form of thin-walled beams, roofs, storage tanks, etc. Due to their specific geometric properties, the application of general doubly curved shell models is inefficient in comparison with the reduced models, specifically designed for singly curved shells.

One of the well-established methods for the analysis of such structures is the finite strip method (FSM) which discretizes cross section with polynomials and approximates fields in longitudinal direction with trigonometric series [1], [2]. Recently, the isogeometric analysis (IGA) is combined with the FSM in a way to discretize the cross section with the NURBS functions, which returned the finite-strip isogeometric (FSIGA) formulation [3]. The method is successfully applied in [4] for the analysis of singly curved shells that are simply supported on both ends.

In this paper, the FSIGA is improved so that it can model clamped-clamped boundary conditions. To avoid classic free-vibration mode shapes of a clamped-clamed beam which consist of hyperbolic functions, a different series is utilized, employing only trigonometric functions [5], [6]. In this way, the numerical issues, inherent for the hyperbolic functions, are avoided.

Brief review of the FSIGA and its application to thin singly curved shells is given in the next section. The numerical analysis and conclusions are delivered in the last two sections.

2. FINITE STRIP ISOGEOMETRIC FORMULATION FOR A SINGLY CURVED SHELL

2.1. METRIC OF THE MIDSURFACE

The present analysis is conducted using the convective frame of reference while the complete shell kinematics is defined by the Cartesian components of translation of midsurface.

The boldface lowercase and uppercase letters are used for vectors and tensors/matrices, respectively. The asterisk symbol designates a deformed configuration while the overbar indicates an equidistant surface. The quantities measured with respect to the local, curvilinear, coordinates are labeled with the caret symbol. The Greek index letters take values of 1 and 2 while the Latin indices take values of 1, 2, and 3. The covariant and partial derivatives with respect to the m^{th} coordinate are designated with $(\,)_{|m}$ and $(\,)_{,m}$, respectively.

The displacement vector of the shell midsurface is $\mathbf{r}=\{x=x^1,\ y=x^2,\ z=x^3\}$, Fig. 1, which is here expressed as a tensor product of two families of lines:

$$\mathbf{r}=\mathbf{r}(\xi,\eta)=x^k\mathbf{i}_k=\sum_{I=1}^{N}R_I(\xi)\sum_{J=1}^{M}F_J(\eta)\mathbf{r}_{IJ},\quad x^k=\sum_{I=1}^{N}R_I(\xi)\sum_{J=1}^{M}f_J^k(\eta)x_{IJ}^k,\quad \mathbf{r}_{IJ}=x_{IJ}^k\mathbf{i}_k, \tag{1}$$

where $R_I(\xi)$ is NURBS basis function of I^{th} control point. $F_J(\eta)$ is J^{th} term of a series, which for the approximation of reference geometry of singly curved shells reduces to the ones used in the semi-analytical FSM, [6]:

$$F_J=\{f_J^1,\ f_J^2,\ f_J^3\}=\{1,\eta,1\}. \tag{2}$$

$\mathbf{r}_{IJ}$ is the position vector of the I^{th} control point for the J^{th} series term, N is the total number of control points along the ξ direction while M is the total number of series terms. $\mathbf{i}_m$ are the base vectors of the Cartesian coordinate system and $\theta^1=\xi$ is local curvilinear coordinate, see Fig. 1.

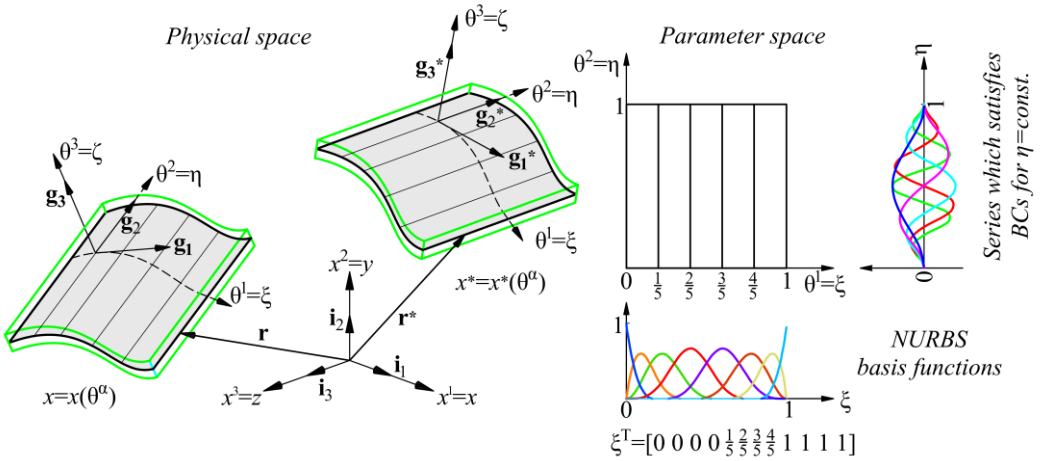

Figure 1. *An isogeometric finite strip model. The mapping between the reference and deformed configurations in physical space (left), and parameter space (right). An example of general basis functions is shown next to the parameter space.*

The base vectors of the midsurface are:

$$\mathbf{g}_1 = \{x^1_{,1}, 0, x^3_{,1}\},\ \ \mathbf{g}_2 = \{0,1,0\},\ \ \mathbf{g}_3 = \{x^1_{,3}, 0, x^3_{,3}\}, \tag{3}$$

where $x^m_{,n}$ are the partial derivatives of the midsurface position with respect to θ^n coordinates. For the adopted description of geometry, components of the base vector $\mathbf{g}_1$ are:

$$x^k_{,1} = \sum_{I=1}^{N}\sum_{J=1}^{M}[R_{I,1}(\xi)\, f^k_J(\eta)]\, x^k_{IJ}. \tag{4}$$

Since the second and the third coordinates, $\theta^2 = \eta$ and $\theta^3 = \zeta$, are straight lines, the base vectors $\mathbf{g}_2$ and $\mathbf{g}_3$, and its reciprocal counterparts $\mathbf{g}^2$ and $\mathbf{g}^3$ are the same and have unit length. The third coordinate $\theta^3 = \zeta$ is orthogonal to the θ^α coordinates and the base vector $\mathbf{g}_3$ represents the normal of a midsurface:

$$\mathbf{g}_3 = \mathbf{g}^3 = \mathbf{n} = \frac{1}{\sqrt{g}}(\mathbf{g}_1 \times \mathbf{g}_2) = x^m_{,3}\,\mathbf{i}_m,\ \ x^m_{,3} = x_{m,3} = \frac{1}{\sqrt{g}} x^k_{,1} x^l_{,2} e_{klm} = -x^3_{,1}\,\mathbf{i}_1 + x^1_{,1}\,\mathbf{i}_3, \tag{5}$$

where e_{mnk} is the permutation symbol and g is the determinant of metric tensor of midsurface:

$$g_{ij} = x^k_{,i} x_{k,j} = \begin{bmatrix} x^m_{,1} x_{m,1} & 0 & 0 \\ 0 & 1 & 0 \\ 0 & 0 & 1 \end{bmatrix},\ \ g = \det g_{ij} = g_{11}. \tag{6}$$

The reciprocal metric tensor of midsurface is:

$$g^{ij} = g_{ij}^{-1} = \frac{1}{g}\begin{bmatrix} 1 & 0 & 0 \\ 0 & g_{11} & 0 \\ 0 & 0 & g_{11} \end{bmatrix} = \begin{bmatrix} g^{11} & 0 & 0 \\ 0 & 1 & 0 \\ 0 & 0 & 1 \end{bmatrix},\ \ \det g^{ij} = 1/g, \tag{7}$$

and the reciprocal tangent vector $\mathbf{g}^1$ is:

$$\mathbf{g}^1 = \frac{1}{\sqrt{g}}(\mathbf{g}_2 \times \mathbf{g}_3) = x^1_n \mathbf{i}^n,\ \ x^1_n = \frac{1}{\sqrt{g}} x^m_{,2} x^k_{,3} e_{mkn} = x^3_{,3}\,\mathbf{i}_1 - x^1_{,3}\,\mathbf{i}_3. \tag{8}$$

The derivatives of the base vector $\mathbf{g}_1$ are calculated as:

$$\mathbf{g}_{1,\alpha} = x^m_{,1\alpha}\mathbf{i}_m = \begin{cases} x^m_{,1\alpha}x_{m,k}\mathbf{g}^k = \Gamma_{1\alpha k}\mathbf{g}^k \\ x^m_{,1\alpha}x^{,n}_{m}\mathbf{g}_n = \Gamma^n_{1\alpha}\mathbf{g}_n \end{cases} \Rightarrow \Gamma^n_{1\alpha} = g^{nk}\Gamma_{1\alpha k}, \tag{9}$$

where $\Gamma_{1\alpha k}$ and $\Gamma^n_{1\alpha}$ are the Christoffel symbols of the first and the second kind, respectively. For the introduced tensor product, Eq. **Error! Reference source not found.**, these derivatives are, [3]:

$$\mathbf{g}_{1,\alpha} = \sum_{I=1}^{N}[\delta^1_\alpha R_{I,11}(\xi)\sum_{J=1}^{M}F_J(\eta)\mathbf{r}_{IJ} + \delta^2_\alpha R_{I,1}(\xi)\sum_{J=1}^{M}F_{J,2}(\eta)\mathbf{r}_{IJ}]. \tag{10}$$

The Christoffel symbols $\Gamma^3_{1\alpha}$ are the components of the curvature tensor and we will mark them as $\Gamma^3_{\alpha\beta} = b_{\alpha\beta}$:

$$\mathbf{g}_{3,\alpha} = -\Gamma^\mu_{3\alpha}\mathbf{g}_\mu = -b^\mu_\alpha\mathbf{g}_\mu, \quad b^\mu_\alpha = g^{\mu\nu}b_{\nu\alpha}, \tag{11}$$

where b^μ_α and $b_{\nu\alpha}$ are the mixed and covariant components of the curvature tensor, respectively, [3]. For singly curved shells, components of the curvature tensor at initial configuration are, Fig. 1:

$$b^1_1 \neq 0, \quad b^2_2 = b^1_2 = b^2_1 = 0. \tag{12}$$

2.2. METRIC OF THE EQUIDISTANT SURFACE

The position vector of an equidistant surface is:

$$\bar{\mathbf{r}} = \mathbf{r} + \zeta\mathbf{g}_3, \tag{13}$$

while its base vectors are:

$$\begin{aligned} &\bar{\mathbf{g}}_1 = \frac{\partial\bar{\mathbf{r}}}{\partial\theta^1} = \mathbf{g}_1 - \zeta b^\nu_1\mathbf{g}_\nu = (\delta^\nu_1 - \zeta b^\nu_1)\mathbf{g}_\nu = \bar{C}^\nu_1\mathbf{g}_\nu, \quad \bar{C}^1_1 = 1-\zeta b^1_1, \quad \bar{C}^2_1 = 0, \\ &\bar{\mathbf{g}}_2 = \mathbf{g}_2, \quad \bar{\mathbf{g}}_3 = \mathbf{g}_3, \end{aligned} \tag{14}$$

where the only non-zero component of *the shift tensor* which is $\bar{C}^\nu_1$ [7]. The covariant metric tensor at an equidistant surface is:

$$\bar{g}_{ij} = \bar{x}^k_{,i}\bar{x}_{k,j} = \begin{bmatrix} \bar{x}^m_{,1}\bar{x}_{m,1} & 0 & 0 \\ 0 & 1 & 0 \\ 0 & 0 & 1 \end{bmatrix}, \quad \bar{g} = \det\bar{g}_{ij} = \bar{g}_{11} = \left(1-\zeta b^1_1\right)^2 g_{11} \approx g_{11} - 2\zeta b_{11}, \tag{15}$$

In the previous equation the quadratic term with respect to ζ coordinate is neglected, which is often for thin and moderately thick shells, [8].

2.3. KIRCHHOFF-LOVE THEORY OF A SINGLY CURVED SHELL

The deformed midsurface is defined with the position vector:

$$\mathbf{r}^* = \mathbf{r} + \mathbf{u}, \tag{16}$$

where the displacement **u** is approximated with the tensor product of the NURBS functions and a series which satisfies boundary conditions for η=const. Here, this series is the same as that used for the description of the geometry, Eq. (1):

$$\mathbf{u} = u^m\mathbf{i}_m = \sum_{I=1}^{N}R_I(\xi)\sum_{J=1}^{M}F_J(\eta)\mathbf{u}_{IJ}, \quad u^m = \sum_{I=1}^{N}R_I(\xi)\sum_{J=1}^{M}f^m_J(\eta)u^m_{IJ}. \tag{17}$$

$\mathbf{u}_{IJ}$ is the vector of displacement components of the I^{th} control point for the J^{th} series term. It can be written as:

$$\mathbf{u} = \mathbf{N}\mathbf{q} \tag{18}$$

where **N** is the matrix of basis functions defined in [4].
The acceleration field is obtained as the second material derivative of the displacement field:

$$\ddot{\mathbf{u}} = \ddot{u}^n \mathbf{i}_n = \mathbf{N}\ddot{\mathbf{q}} \tag{19}$$

According to the KL hypothesis, the expressions for the reference strains of the midsurface for singly curved shells within the scope of the linear theory are, [4]:

$$\begin{aligned}
&\varepsilon_{11} = x_{k,1}u^k_{,1} = x_{1,1}u^1_{,1} + x_{3,1}u^3_{,1},\\
&\varepsilon_{22} = x_{k,2}u^k_{,2} = u^2_{,2},\\
&2\varepsilon_{12} = x_{k,2}u^k_{,1} + x_{k,1}u^k_{,2} = u^2_{,1} + x_{1,1}u^1_{,2} + x_{3,1}u^3_{,2},\\
&\kappa_{11} = x_{k,3}(u^k_{,11} - \Gamma^\mu_{11}u^k_{,\mu}) = x_{1,3}u^1_{,11} + x_{3,3}u^3_{,11} - \Gamma^1_{11}(x_{1,3}u^1_{,1} + x_{3,3}u^3_{,1}),\\
&\kappa_{22} = x_{k,3}(u^k_{,22} - \Gamma^\mu_{22}u^k_{,\mu}) = x_{1,3}u^1_{,22} + x_{3,3}u^3_{,22},\\
&2\kappa_{12} = 2x_{k,3}(u^k_{,12} - \Gamma^\mu_{12}u^k_{,\mu}) = 2(x_{1,3}u^1_{,12} + x_{3,3}u^3_{,12}).
\end{aligned} \tag{20}$$

while the relations between the equidistant and reference strains are:

$$\bar{\varepsilon}_{\alpha\beta} = \varepsilon_{\alpha\beta}(\zeta) = \frac{1}{2}(\bar{g}^*_{\alpha\beta} - \bar{g}_{\alpha\beta}) \approx \frac{1}{2}(g^*_{\alpha\beta} - g_{\alpha\beta}) - \zeta(b^*_{\alpha\beta} - b_{\alpha\beta}) = \varepsilon_{\alpha\beta} - \zeta\kappa_{\alpha\beta}. \tag{21}$$

The stress-strain relation is defined with the classic Saint Venant-Kirchhoff material model for the plane stress and plane strain conditions:

$$\sigma^{\alpha\beta} = 2\mu(g^{\alpha\nu}g^{\beta\gamma} + \frac{\nu}{1-\nu}g^{\alpha\beta}g^{\nu\gamma})\varepsilon_{\nu\gamma} = D^{\alpha\beta\nu\gamma}\varepsilon_{\nu\gamma}, \tag{22}$$

where $D^{\alpha\beta\nu\gamma}$ are the components of the constitutive tensor while μ and ν are Lamé constants.

2.4. PRINCIPLE OF VIRTUAL WORK

The principle of virtual work, when the external effects are neglected, can be written as:

$$\delta W = \int_v \bar{\sigma}^{ij}\delta\bar{\varepsilon}_{ij}dv + \int_v \rho\ddot{\bar{u}}^i\delta\bar{u}_i dv = \int_v \bar{\boldsymbol{\sigma}} : \delta\bar{\boldsymbol{\varepsilon}}\, dv + \int_v \rho\ddot{\bar{\mathbf{u}}}\cdot\delta\bar{\mathbf{u}}\, dv = 0, \tag{23}$$

where **σ** is the Cauchy stress tensor, **ε** is the strain tensor, and **ü** is the vector of accelerations. After integration of Eq. (23) along the thickness, the internal term reduces to:

$$\int_v \bar{\sigma}^{\alpha\beta}\delta\bar{\varepsilon}_{\alpha\beta}\mathrm{d}v = \int_a (N^{\mu\nu}\delta\varepsilon_{\mu\nu} + M^{\mu\nu}\delta\kappa_{\mu\nu})\mathrm{d}a, \tag{24}$$

where $N^{\mu\nu}$ and $M^{\mu\nu}$ are the stress resultants and stress couples which are energetically conjugated with the reference strains of the midsurface, $\varepsilon_{\mu\nu}$ and $\kappa_{\mu\nu}$.

By assuming that the material is homogenous and that the effect of rotational inertia is negligible, the inertial term of virtual work reduces to:

$$\int_v \rho\ddot{\bar{u}}^i\delta\bar{u}_i dv = \rho h\int_a \ddot{u}^i\delta u_i da. \tag{25}$$

Now, Eq. (23) can be written in matrix form as:

$$\delta W = \int_a \mathbf{f}^{\mathrm{T}}\delta\mathbf{e}\,\mathrm{d}a + \rho h\int_a \ddot{\mathbf{u}}^{\mathrm{T}}\delta\mathbf{u}\,\mathrm{d}a = 0, \tag{26}$$

where $\mathbf{f}^{\mathrm{T}}$ and $\mathbf{e}^{\mathrm{T}}$ are the the vectors of generalized section forces and reference strains of the shell midsurface:

$$\begin{aligned}
\mathbf{f}^{\mathrm{T}} &= \begin{bmatrix} N^{11} & N^{22} & N^{12} & M^{11} & M^{22} & M^{12} \end{bmatrix},\\
\mathbf{e}^{\mathrm{T}} &= \begin{bmatrix} \varepsilon_{11} & \varepsilon_{22} & 2\varepsilon_{12} & \kappa_{11} & \kappa_{22} & 2\kappa_{12} \end{bmatrix}.
\end{aligned} \tag{27}$$

The constitutive relations between the energetically conjugated section forces and reference strains can be represented in a compact form as:

$$\mathbf{f} = \mathbf{D}\mathbf{e}, \tag{28}$$

where **D** is the constitutive tensor:

$$\mathbf{D}=\begin{bmatrix}\mathbf{D}_M & \mathbf{0}\\ \mathbf{0} & \mathbf{D}_B\end{bmatrix}=\begin{bmatrix}D_M^{\alpha\beta\gamma\lambda} & 0\\ 0 & D_B^{\alpha\beta\gamma\lambda}\end{bmatrix}\mathbf{g}_\alpha\otimes\mathbf{g}_\beta\otimes\mathbf{g}_\gamma\otimes\mathbf{g}_\lambda. \tag{29}$$

2.5. DISCRETE EQUATION OF MOTION

The relation between the reference strains and the displacements of control points for one isogeometric finite strip can be represented with the strain-displacement matrix **B**, defined in [4]:

$$\mathbf{e}=\mathbf{B}\mathbf{q}=\mathbf{L}\mathbf{H}\mathbf{q}, \tag{30}$$

and Eq. (26) can be written as:

$$\delta W=\int_a \mathbf{e}^{\mathrm{T}}\mathbf{D}\delta\mathbf{e}\,\mathrm{d}a+\rho h\int_a\ddot{\mathbf{u}}^{\mathrm{T}}\delta\mathbf{u}\,\mathrm{d}a=\mathbf{q}^{\mathrm{T}}\int_a\mathbf{B}^{\mathrm{T}}\mathbf{D}\mathbf{B}\,\mathrm{d}a\delta\mathbf{q}+\rho h\ddot{\mathbf{q}}^{\mathrm{T}}\int_a\mathbf{N}^{\mathrm{T}}\mathbf{N}\,\mathrm{d}a\delta\mathbf{q}=0, \tag{31}$$

or:

$$\begin{aligned}&\mathbf{M}\ddot{\mathbf{q}}+\mathbf{K}\mathbf{q}=0,\\ &\mathbf{K}=\int_a\mathbf{B}^{\mathrm{T}}\mathbf{D}\mathbf{B}\,\mathrm{d}a,\quad \mathbf{M}=\rho h\int_a\mathbf{N}^{\mathrm{T}}\mathbf{N}\,\mathrm{d}a,\end{aligned} \tag{32}$$

where **K** and **M** are the stiffness and mass matrices of one isogeometric finite strip, respectively. Solving the equation (32) yields a well-known eigenvalue problem:

$$\left(\mathbf{K}-\omega^2\mathbf{M}\right)\tilde{\mathbf{q}}=\mathbf{0}, \tag{33}$$

with 3*NM* nontrivial solutions of eigenpairs of eigenfrequencies ω_i and corresponding eigenvectors $\tilde{\mathbf{q}}_i$.

2.6. SERIES PART OF BASIS FUNCTION

The presented FSIGA, applied to the analysis of singly curved shells, uses series only for the kinematic field. This is analogous to the semi-analytical FSM that enables modeling of all types of classic boundary conditions, [2, 6]. Here, only the clamped-clamped boundary conditions are considered.

It is convenient to utilize two different series. One approximates the two components of a displacement vector in a transverse plane of a shell while the other series approximates the longitudinal (along the η-axis) component of a displacement vector, Fig. 1 [6]. If the longitudinal ends of a strip are clamped, a simple choice for the basis functions f^1 and f^3 is suggested in [5]:

$$f_J^1=f_J^3=\sin\left(J\pi\eta/L\right)\sin\left(\pi\eta/L\right),\quad J=1,2,...M, \tag{34}$$

which satisfies boundary conditions: $\hat{u}^1(\xi,0)=\hat{u}^1(\xi,L)=\hat{u}^3(\xi,0)=\hat{u}^3(\xi,L)=0$ and $\hat{u}^1_{,2}(\xi,0)=\hat{u}^1_{,2}(\xi,L)=\hat{u}^3_{,2}(\xi,0)=\hat{u}^3_{,2}(\xi,L)=0$. Regarding the approximation of displacement component along the longitudinal direction, a simple sine series is considered:

$$f_J^2=\sin\left(J\pi\eta/L\right),\quad J=1,2,...M, \tag{35}$$

Let us simplify the notation with: $f_m^1=f_m^3=Z_m$, $f_m^2=Y_m$. In this way, the thirteen integrals with respect to the series terms which should be solved in the Eq. (32) are:

$$
\begin{aligned}
&I_{1mn}=\int_0^L Z_m Z_n d\eta,\ I_{2mn}=\int_0^L Z_{m,22} Z_n d\eta,\ I_{3mn}=\int_0^L Z_{m,22} Z_{n,22} d\eta,\ I_{4mn}=\int_0^L Z_{m,2} Z_{n,2} d\eta,\\
&I_{5mn}=\int_0^L Y_{m,2} Z_n d\eta,\ I_{6mn}=\int_0^L Y_m Z_{n,2} d\eta,\ I_{7mn}=\int_0^L Y_{m,2} Y_{n,2} d\eta,\\
&I_{8mn}=\int_0^L Y_m Y_n d\eta,\ I_{9mn}=\int_0^L Z_{m,22} Z_{n,2} d\eta,\ I_{10mn}=\int_0^L Z_{m,22} Y_{n,2} d\eta,\\
&I_{11mn}=\int_0^L Z_{m,2} Y_{n,2} d\eta,\ I_{12mn}=\int_0^L Y_m Z_n d\eta,\ I_{13mn}=\int_0^L Z_{m,2} Y_n d\eta.
\end{aligned}
\tag{36}
$$

The integration of trigonometric functions is here done analytically, cf. Appendix.

3. NUMERICAL EXAMPLES

The aim of the present numerical analysis is to verify and validate the developed FSIGA regarding the singly curved shells with clamped-clamped boundary conditions, and to examine its convergence properties. The numerical reference solutions obtained with highly refined FSIGA meshes are utilized in each experiment. A designation for an IGFSM mesh is *m*h-*n*p-*i*k-*j*t, where *m*, *n*, *i*, and *j* are the number of strips (knot spans), the order of NURBS, the interstrip continuity, and the number of series terms, respectively.

The validation tests are done by the comparison with the results found with dense uniform meshes of STRI3 shell elements. This element is the only one in the Abaqus library which imposes KL constraints analytically, [9].

Additional comparison is made with the standard flat shell finite strips LO2 and HO3 [1, 6].

3.1 AN OPEN CIRCULAR CYLINDER

An open circular cylinder as in Fig. 2 is studied first. The reference FSIGA frequencies for the first eight modes are calculated with 80h-4p-1k-40t mesh and given in Table. 1 The results obtained with a smaller number of degrees of freedom are presented only for the purpose of comparing with the results found with Abaqus. Excellent accuracy per DOF of the FSIGA is evident. Regarding the mode shapes, they are virtually indistinguishable from those in Abaqus, and only the FSIGA results are visualized, Fig. 3.

The results of *h*-refinement tests are given in Fig. 4. They imply that an increase in the NURBS order and interstrip continuity significantly increases the order of convergence. The convergences of LO2 and HO3 strips are displayed in Fig 5. These flat shell strips have inferior orders of convergence in comparison with the curved NURBS strips of similar order.

The results of *t*-refinement tests for cubics and quartics NURBS with the lowest and the highest continuities are given in Fig. 6 and Fig. 7. Similar orders of convergence are detected for both models, near 2. The same influence of odd and even series terms as in [4] is observed.

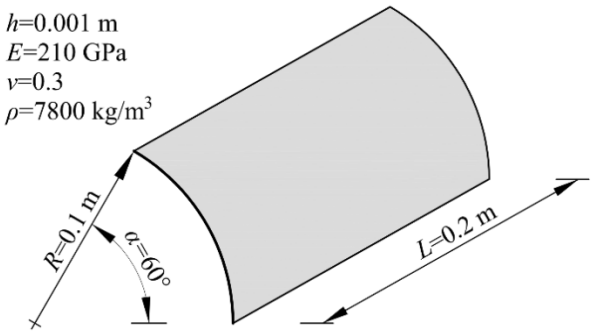

Figure 2. *The open circular cylinder.*

Table 1. The open circular cylinder. Comparison of the lowest eight eigenfrequencies [Hz].

Mode	Abaqus STRI3		Present	
	1680 elements (n_{DOF}=5412)	167200 elements (n_{DOF}=505260)	20h-2p-1k-10t (n_{DOF}=660)	80h-4p-1k-40t (n_{DOF}=29040)
1	523.81	505.62	509.58	506.09
2	577.03	569.19	572.10	569.41
3	1011.7	984.35	989.97	984.84
4	1101.3	1070.7	1079.70	1071.84
5	1555.6	1549.6	1562.99	1550.83
6	1587.3	1564.5	1577.03	1565.26
7	1662.2	1632.1	1655.80	1637.02
8	1689.5	1650.5	1665.76	1652.28

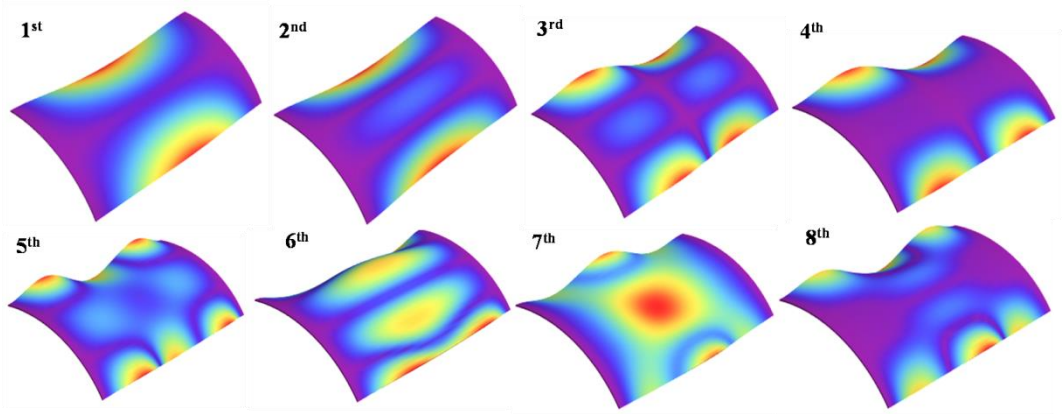

Figure 3. *The open circular cylinder. Mode shapes of the lowest eight modes.*

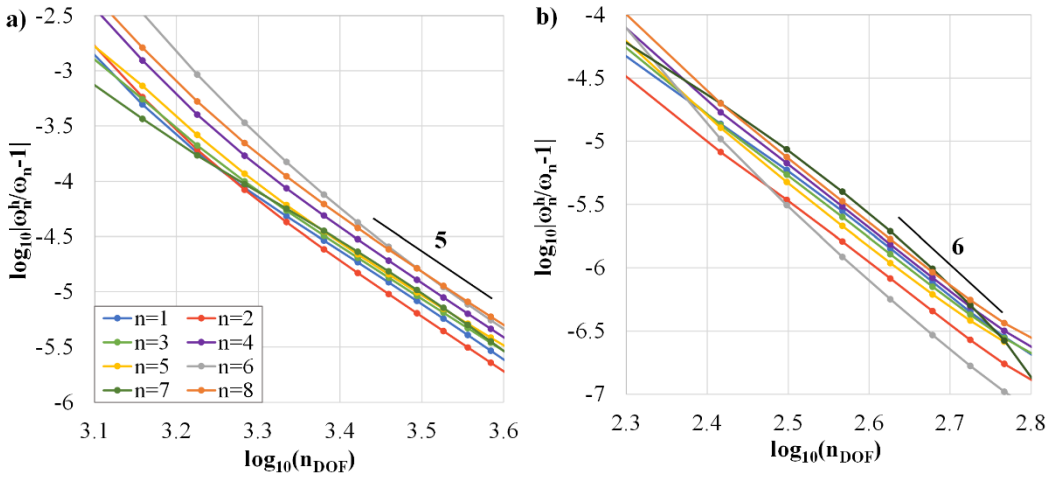

Figure 4. *The open circular cylinder. Convergence of the relative error for the lowest eight eigenfrequencies using the h-refinement: a) mh-3p-2k-40t; b) mh-4p-1k-40t*

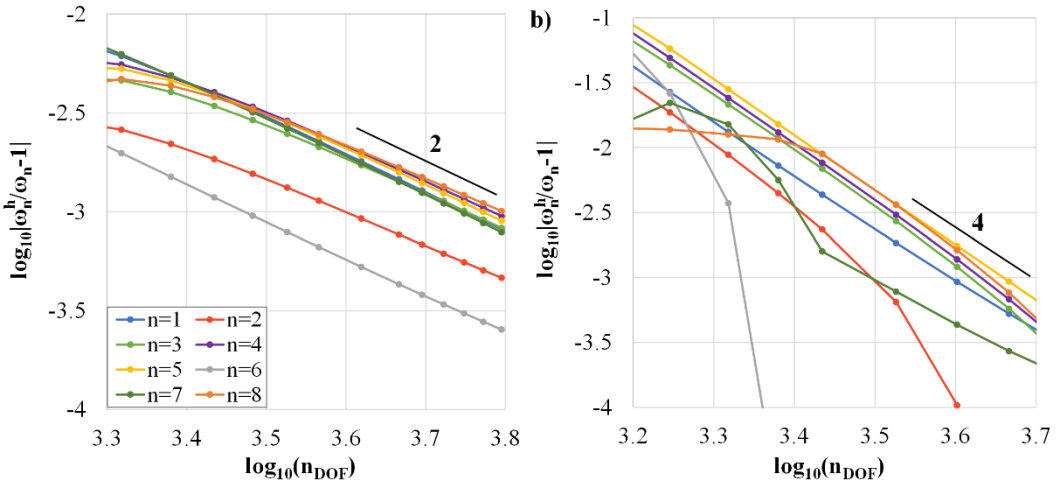

Figure 5. *The open circular cylinder. Convergence of the relative error for the lowest eight eigenfrequencies using the h-refinement and forty series terms: a) LO2 strip; b) HO3 strip.*

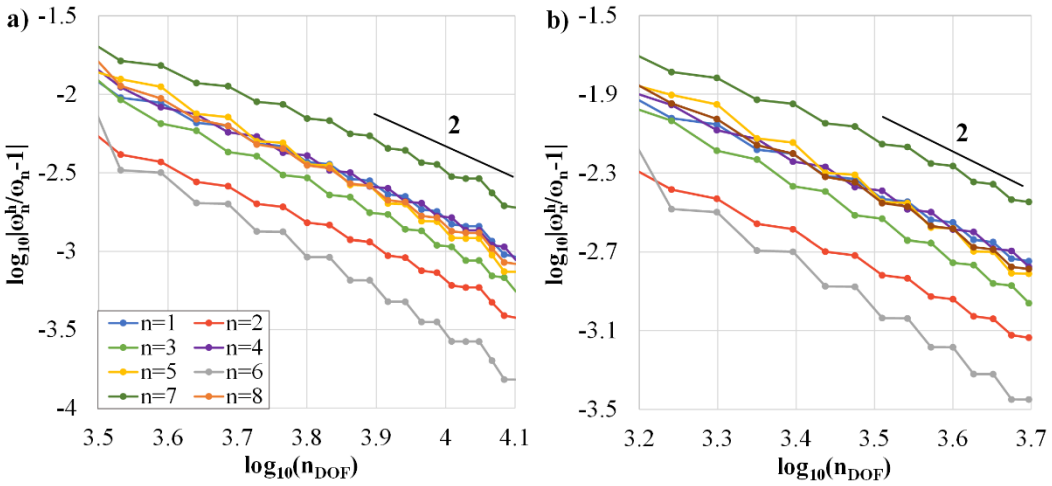

Figure 6. *The open circular cylinder. Convergence of the relative error for the lowest eight eigenfrequencies using the t-refinement: a) 80h-3p-1k-jt; b) 80h-3p-2k-jt*

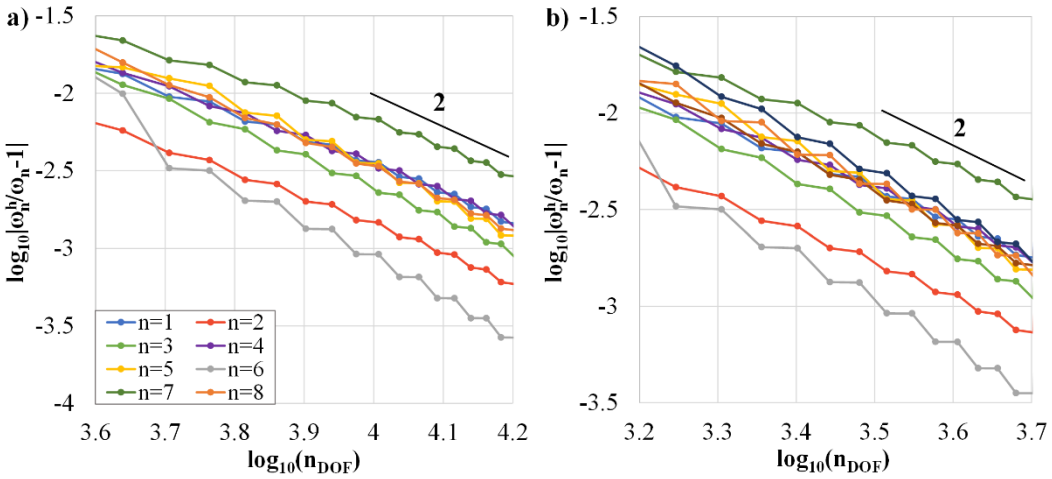

Figure 7. *The open circular cylinder. Convergence of the relative error for the lowest eight eigenfrequencies using the t-refinement: a) 80h-4p-1k-jt; b) 80h-4p-3k-jt*

3.2 A QUARTIC CYLINDER WITH SYMMETRIC CROSS SECTION

In this example we consider a shell with symmetric circumferential profile, described with the quartic NURBS, Fig. 8. Its parametric equations are:

$$x(\xi)=\frac{0.08-0.32\ \xi+1.2\ \xi^2-1.76\ \xi^3+0.88\ \xi^4}{0.2+0.8\ \xi-1.8\ \xi^2+2\ \xi^3-\xi^4},$$
$$z(\xi)=\frac{-0.45\ \xi^2+0.1\ \xi^3+0.25\ \xi^4}{-0.2-0.8\ \xi+1.8\ \xi^2-2\ \xi^3+\xi^4}. \tag{37}$$

The reference mesh is the same as in the previous example, 80h-4p-1k-40t. The lowest eight eigenfrequencies are scrutinized with respect to the results obtained with STRI3 elements in Table 2 while the mode shapes are displayed in Fig. 9.

The convergences of eigenfrequencies with respect to the *h*-refinement are presented in Fig. 10 and Fig. 11. An astonishing improvement of accuracy per DOF is obtained for meshes with increased smoothness. The *t*-refinement results are given in Fig. 12 and Fig. 13. The orders of convergences are similar to those estimated in the previous example, close to 2.

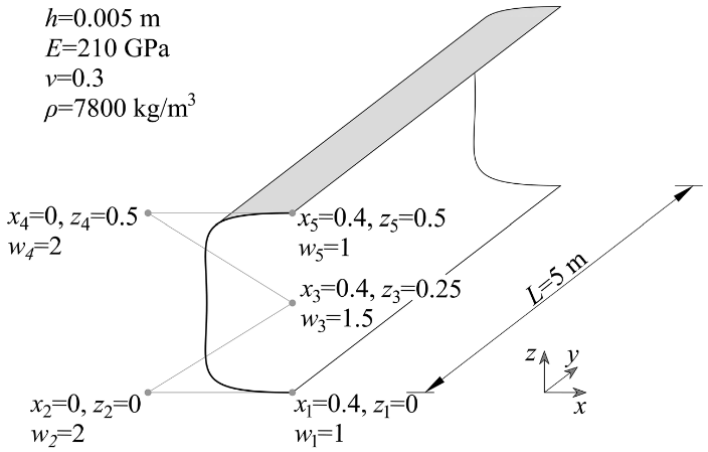

Figure 8. *The quartic cylinder. Geometry and material properties. The weights of control points are designated with* w_i.

Table 2. The quartic cylinder. Comparison of the lowest eight eigenfrequencies [Hz].

	Abaqus STRI3		**Present**	
Mode	1608 elements (n_{DOF}=5304)	89000 elements (n_{DOF}=270540)	20h-4p-1k-10t (n_{DOF}=1860)	80h-4p-1k-40t (n_{DOF}=29040)
1	32.74	32.87	32.89	32.87
2	35.97	33.57	33.93	33.64
3	37.78	36.98	37.04	36.96
4	47.38	44.15	44.30	44.10
5	56.41	54.15	55.24	54.81
6	58.95	55.79	56.42	55.89
7	61.51	56.29	56.47	56.33
8	64.16	63.83	63.99	63.82

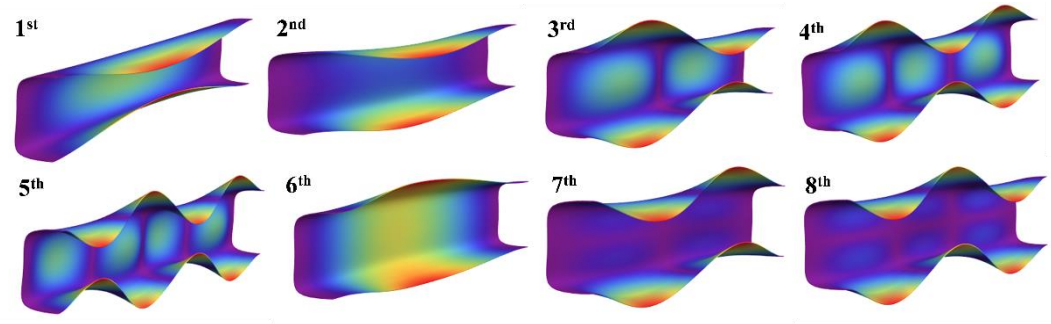

Figure 9. *The quartic cylinder. Mode shapes of the lowest eight modes.*

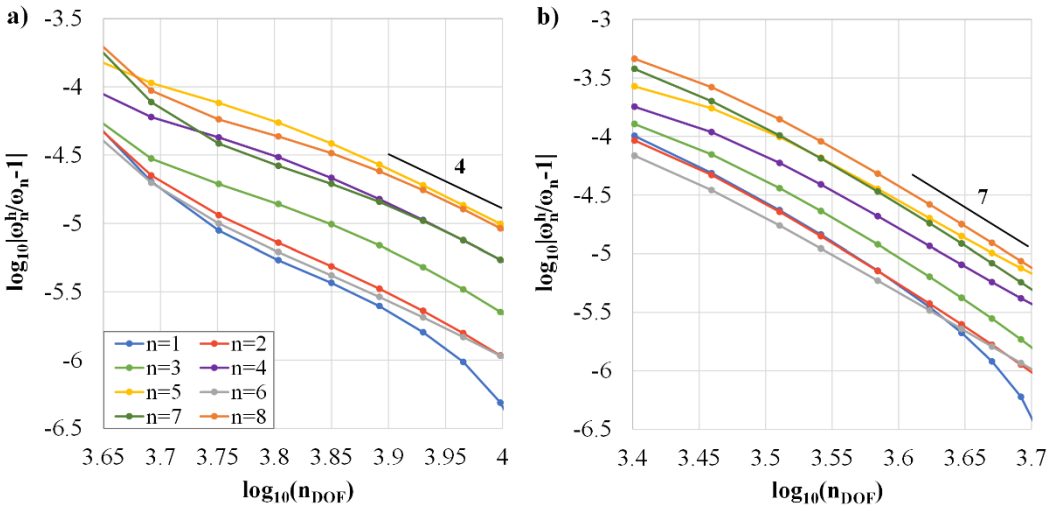

Figure 10. *The quartic cylinder. Convergence of the relative error for the lowest eight eigenfrequencies using the h-refinement: a) mh-4p-1k-40t; b) mh-4p-3k-40t.*

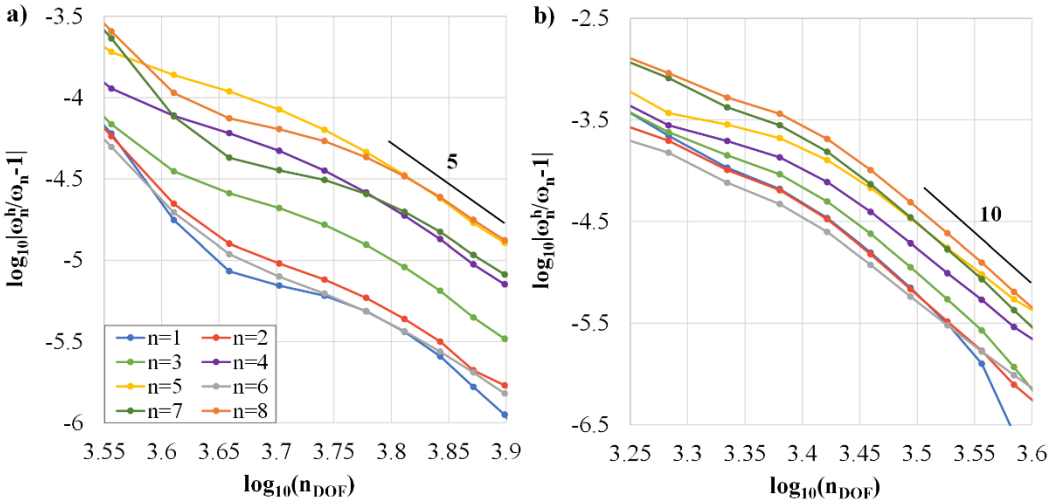

Figure 11. *The quartic cylinder. Convergence of the relative error for the lowest eight eigenfrequencies using the h-refinement: a) mh-5p-1k-40t; b) mh-5p-4k-40t.*

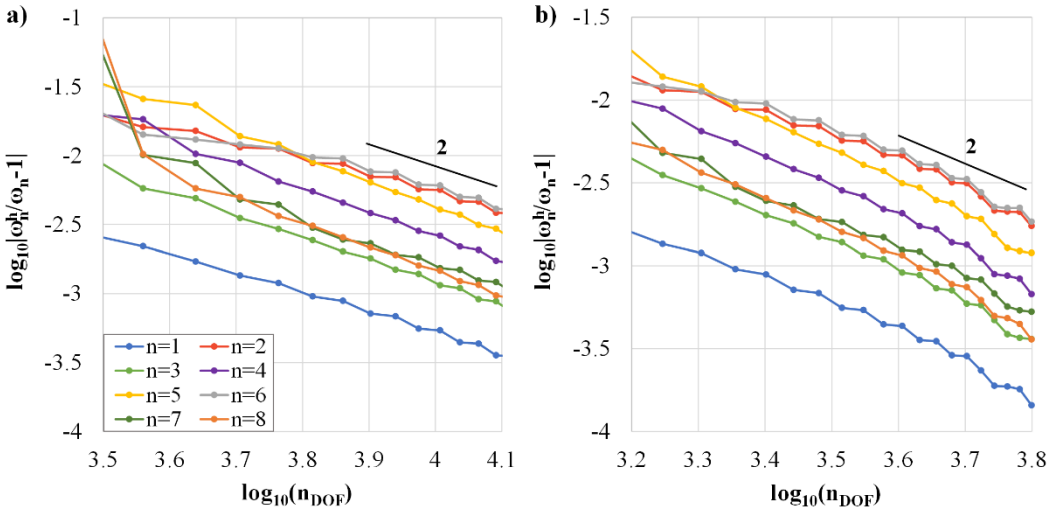

Figure 12. *The quartic cylinder. Convergence of the relative error for the lowest eight eigenfrequencies using the t-refinement: a) 80h-4p-1k-jt; b) 80h-4p-3k-jt.*

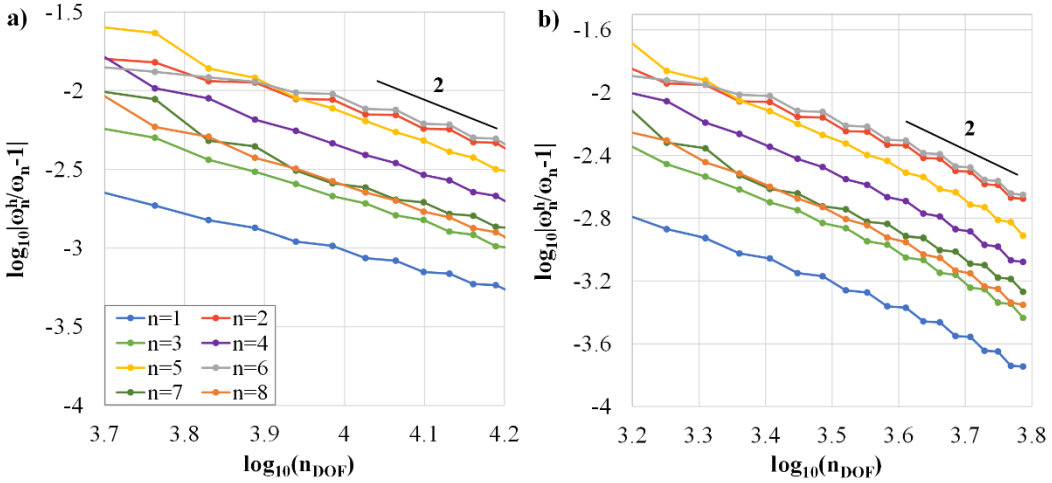

Figure 13. *The quartic cylinder. Convergence of the relative error for the lowest eight eigenfrequencies using the t-refinement: a) 80h-5p-1k-jt; b) 80h-5p-4k-jt.*

4 CONCLUSIONS

The recently developed FSIGA hybrid metod is revised and improved by implementing the clamped-clamped isogeometric finite strip. A pure trigonometric series is used and the numerical issues with hyperbolic functions are avoided. As in the previous work, excellent results are obtained in comparison with the finite element method.

The presented method provides improved orders of convergence and allows the analytical integration of trigonometric functions. Additionally, an arbitrarily curved reference geometry can be exactly represented by the NURBS functions. These properties make the FSIGA well-suited for the analysis of singly curved shells.

ACKNOWLEDGMENTS

A. Borković acknowledges the support of the Austrian Science Fund (FWF): M 2806-N.

Appendix A.

Closed-form solutions of the thirteen integrals in Eq. (36) are given here.

$$I_{1mn}=\begin{cases}\frac{3L}{8}, & m=n=1\\ \frac{L}{4}, & m=n\neq 1\\ -\frac{L}{8}, & |m-n|=2\\ 0, & \text{other}\end{cases},\quad I_{2mn}=\begin{cases}-\frac{\left(1+n^2\right)\pi^2}{4L}, & m=n\\ \frac{\left(1+n\right)^2\pi^2}{8L}, & m=n+2\\ \frac{\left(-1+n\right)^2\pi^2}{8L}, & n=m+2\\ 0, & \text{other}\end{cases},\quad I_{3mn}=\begin{cases}\frac{\left(1+6n^2+n^4\right)\pi^4}{4L^3}, & m=n\\ -\frac{\left(1+n\right)^4\pi^4}{8L^3}, & m=n+2,\\ -\frac{\left(-1+n\right)^4\pi^4}{8L^3}, & n=m+2\\ 0, & \text{other}\end{cases}$$

$$I_{4mn}=\begin{cases}\frac{\left(1+n^2\right)\pi^2}{4L}, & m=n\\ -\frac{\left(1+n\right)^2\pi^2}{8L}, & m=n+2\\ -\frac{\left(-1+n\right)^2\pi^2}{8L}, & n=m+2\\ 0, & \text{other}\end{cases},\quad I_{5mn}=\begin{cases}-\frac{\left(1+n\right)\pi}{4}, & m=n+1\\ \frac{\left(-1+n\right)\pi}{4}, & n=m+1,\\ 0, & \text{other}\end{cases}\quad I_{6mn}=\begin{cases}\frac{\left(1+n\right)\pi}{4}, & m=n+1\\ -\frac{\left(-1+n\right)\pi}{4}, & n=m+1,\\ 0, & \text{other}\end{cases}$$

$$I_{7mn}=\begin{cases}\frac{n^2\pi^2}{2L}, & m=n\\ 0, & m\neq n\end{cases},\quad I_{8mn}=\begin{cases}\frac{L}{2}, & m=n\\ 0, & m\neq n\end{cases},$$

$$I_{9mn}=\begin{cases}-\frac{8\left[-1+\left(-1\right)^{m+n}\right]\left[-3+n^2+m^2\left(1+n^2\right)\right]m\cdot n\cdot\pi^2}{L^2\left(-2+m-n\right)\left(m-n\right)\left(2+m-n\right)\left(-2+m+n\right)\left(m+n\right)\left(2+m+n\right)}, & |m-n|=1,3,5,\text{K}\\ 0, & \text{other}\end{cases},$$

$$I_{10mn}=\begin{cases}-\frac{n^3\pi^3}{4L^2}, & m=n+1\\ \frac{n^3\pi^3}{4L^2}, & n=m+1\\ 0, & \text{other}\end{cases},$$

$$I_{11mn}=\begin{cases}-\frac{2\left[1+\left(-1\right)^{m+n}\right]m\cdot n^3\cdot\pi}{L\left(-1+m-n\right)\left(1+m-n\right)\left(-1+m+n\right)\left(1+m+n\right)}, & |m-n|=0,2,4,\text{K}\\ 0, & \text{other}\end{cases},$$

$$I_{12mn}=\begin{cases}-\frac{2\left[1+\left(-1\right)^{m+n}\right]m\cdot n\cdot L}{\left(-1+m-n\right)\left(1+m-n\right)\left(-1+m+n\right)\left(1+m+n\right)\pi}, & |m-n|=0,2,4,\text{K}\\ 0, & \text{other}\end{cases},$$

$$I_{13mn}=\begin{cases}-\frac{4\left[-1+\left(-1\right)^{m+n}\right]\left(-2+m^2+n^2\right)m\cdot n}{\left(-2+m-n\right)\left(m-n\right)\left(2+m-n\right)\left(-2+m+n\right)\left(m+n\right)\left(2+m+n\right)}, & |m-n|=1,3,5,\text{K}\\ 0, & \text{other}\end{cases}.$$

LITERATURE

[1] Y. Cheung and L. Tham, The finite strip method, CRC Press, 1997.

[2] D. D. Milašinović, The Finite Strip Method in Computational Mechanics, Faculties of Civil Engineering: University of Novi Sad, Technical University of Budapest and University of Belgrade: Subotica, Budapest, Belgrade, 1997.

[3] G. Radenković, Finite rotation and finite strain isogeometric structural analysis (in Serbian), Belgrade: Faculty of Architecture, 2017.

[4] A. Borković, G. Radenković, D. Majstorović, S. Milovanović, D. Milašinović and R. Cvijić, "Free vibration analysis of singly curved shells using the isogeometric finite strip method," *Thin-Walled Structures*, vol. 157, p. 107125, 2020.
[5] M. A. Bradford and M. Azhari, "Buckling of plates with different end conditions using the finite strip method," *Computers & Structures*, vol. 56, no. 1, pp. 75–83, 1995.
[6] A. Borković, S. Kovačević, D. D. Milašinović, G. Radenković, O. Mijatović and V. Golubović-Bugarski, "Geometric nonlinear analysis of prismatic shells using the semi-analytical finite strip method," *Thin-Walled Structures*, vol. 117, pp. 63–88, 2017.
[7] M. Bischoff, K. Bletzinger, W. Wall and E. Ramm, "Models and Finite Elements for Thin-Walled Structures," *Encyclopedia of Computational Mechanics*, 2004.
[8] J. Kiendl, M.-C. Hsu, M. C. H. Wu and A. Reali, "Isogeometric Kirchhoff–Love shell formulations for general hyperelastic materials," *Computer Methods in Applied Mechanics and Engineering*, vol. 291, pp. 280–303, 2015.
[9] *Abaqus Documentation*. Dassault Systèmes, 2014.